

Optical Properties of Nanostructured Optical Materials

Russell J. Gehr* and Robert W. Boyd

Institute of Optics, University of Rochester, Rochester, New York 14627

Received February 1, 1996. Revised Manuscript Received April 24, 1996[®]

The optical properties of nanoscale composite materials are often quite different from the properties of the constituent materials from which the composite is constructed. The formation of composite materials thus constitutes a means for engineering new materials with desired optical properties. In this paper we review theories and models that have been devised for relating the linear and nonlinear optical properties of composite materials to those of the constituent materials and to the morphology of the composite structure, and we review experimental studies aimed at validating these models. Morphologies that are explicitly discussed include those of Maxwell Garnett and of Bruggeman, layered structures, and fractal structures.

1. Introduction

The optical properties of composite materials comprise an interesting field of study, since these properties may differ significantly from those of the constituents. Due to this fact it is conceivable that one may actually design materials with properties meeting a set of desirable conditions. To achieve this goal, two requirements must be met: suitable constituent materials must be found and characterized and relationships predicting the effective optical parameters of a composite must be determined. The former problem is being actively addressed by materials scientists, especially in the areas of polymers and semiconductors. It is the latter problem that will be addressed in this article.

Before beginning the discussions about the various models of composites, we must define what is meant by the term "composite". Obviously, there are a number of possibilities. For this article we will confine ourselves to this one: a composite is any material which is formed from two or more different constituents with the following size constraint. Each constituent is present in the whole in grains large enough that it may be described by its bulk optical properties. At the same time the typical grain dimensions and spacings must be much smaller than an optical wavelength so that the composite may be described by effective optical parameters which are related to the constituent parameters.

An example of such a composite is stained glass, i.e., glass doped with small metal particles. The dimensions of the particles are typically on the order of hundreds of angstroms, which is much smaller than optical wavelengths. (On the other hand, some stained glasses have such small dopings of the metal that the spacing between particles may be comparable to a wavelength. These glasses may not be well described by effective medium theory.) It is obvious that such composites have significantly different properties than their constituents. The glass is nonabsorbing throughout the visible spectrum, the metal is highly absorbing and reflective throughout the same range, but the composite displays a resonance absorption peak within the visible, which gives the glass its characteristic coloring. In an

effort to explain this phenomenon, Maxwell Garnett¹ developed one of the earliest effective medium theories. His efforts, which will be described in detail later in this paper, were very successful; the effective dielectric constant he derived accurately predicted the location of the resonance in the visible part of the spectrum.

The task of determining the effective linear and nonlinear optical constants of a composite may be performed either theoretically or empirically. Theoretical analyses are in general difficult to perform with solutions possible only in certain special cases. For those composite geometries which lend themselves to analytic solutions, it then becomes an easier problem to tailor materials; the constituent parameters necessary to achieve the desired composite parameters become well-known. However, it may still be a difficult problem finding materials with these characteristics and combining them in the necessary manner.

The aim of this paper is to review the work that has been performed on composite materials, with an emphasis on the determination of their optical properties. The manufacture of the composites will not be considered, although many of the references cited herein do give some details regarding these processes.

Before considering specific composite geometries, it is informative to ask the question, How much can we determine theoretically about such composites without knowledge of the underlying geometry? The answer is that it is not possible to predict the effective medium parameters, but it is possible to determine upper and lower limits on the effective linear dielectric constant. This was shown by Brown,² who considered the problem of a two-constituent composite using a statistical approach. He derived an integral equation for the macroscopic polarization of the composite and then used successive Born approximations to determine the effective dielectric constant. The first two terms in his expression were independent of the geometry of the composite, but all subsequent terms required knowledge of the mesoscopic structure.

So how restrictive a set of limits may be found? Obviously, the value of the effective dielectric constant must fall between the maximum and minimum values of the dielectric constants of the constituents. It is

* Abstract published in *Advance ACS Abstracts*, July 15, 1996.

possible to do better than this. The most well-known limits are the Wiener limits³ derived for composites whose constituents have purely real dielectric constants:

$$\sum_i f_i \epsilon_i \geq \epsilon_{\text{eff}} \geq [\sum_i f_i / \epsilon_i]^{-1} \quad (1)$$

An intuitive explanation of these limits may be garnered from the analogous problem of determining the effective electrical conductivity of a composite. The expression for the Wiener limits is identical, with the dielectric constant ϵ replaced by the conductivity σ . In this case one can picture the composite as a network of conductors connected in series and parallel. The maximum conductivity achievable occurs when all of the elements in the network are connected in parallel; the minimum conductivity achievable occurs when all of the elements are connected in series. The effective conductivity will fall somewhere between these bounds, which are exactly the Wiener limits.

It is possible to determine more restrictive limits than the Wiener limits. Hashin and Shtrikman⁴ explored the problem, using only the assumptions that the composite is macroscopically homogeneous and isotropic. Using a variational approach, they determined the most restrictive limits that can be found under these simple assumptions. For a two-constituent composite their result is

$$\epsilon_1^* \leq \epsilon_{\text{eff}} \leq \epsilon_2^* \quad (2)$$

where

$$\epsilon_1^* \equiv \epsilon_1 + f_2 / \left(\frac{1}{\epsilon_2 - \epsilon_1} + \frac{f_1}{3\epsilon_1} \right) \quad (3)$$

$$\epsilon_2^* \equiv \epsilon_2 + f_1 / \left(\frac{1}{\epsilon_1 - \epsilon_2} + \frac{f_2}{3\epsilon_2} \right) \quad (4)$$

and f_1 and f_2 are the volume fill fractions of constituents 1 and 2, respectively, and it is assumed that $\epsilon_1 < \epsilon_2$.

Bergman⁵ pointed out that there is a way to find more restrictive limits without knowing the actual composite microstructure. If some macroscopic parameter other than the dielectric constant is known for the composite, it gives us information about the geometry of the composite. Thus it is possible to use this information in the variational analysis to derive even tighter bounds.

These results, while interesting, do not provide a complete solution to the problem at hand. We wish to know the values of the effective medium parameters. Thus we must consider specific composite geometries. In the next section we discuss the Maxwell Garnett geometry and some of its modifications. In subsequent sections we discuss the Bruggeman geometry (randomly interspersed media), the layered geometry, and fractal structures.

2. Maxwell Garnett Geometry Composites

The composite geometry most often considered both theoretically and experimentally consists of inclusion particles randomly dispersed in a host material (see Figure 1). This composite was considered by Maxwell Garnett,¹ who attempted to explain the linear optical properties of metal-doped glasses. His model assumed that the inclusion particles were spherical and uniform in size. Under the assumption that the inclusion radius was much smaller than the typical spacing between

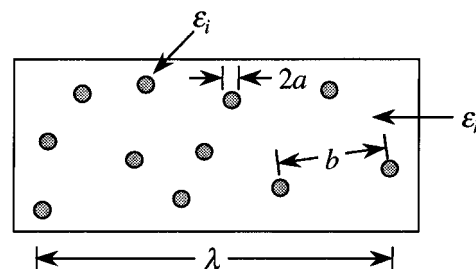


Figure 1. Maxwell Garnett composite geometry.

inclusions, which in turn was much smaller than an optical wavelength, an effective dielectric constant could be determined for the composite. Observing that a metal sphere in the presence of an oscillating electric field emits radiation as if it were an electric dipole, Maxwell Garnett replaced the spheres in the model by the equivalent point dipoles, i.e., he ignored their finite size. If \mathbf{p} represents the average dipole moment of an inclusion and N represents the number of inclusions per unit volume, then the total polarization of the medium (normalized by the dielectric constant of the host) is given by

$$\mathbf{P} = N\mathbf{p} \quad (5)$$

The average dipole moment is given by

$$\mathbf{p} = a^3 \frac{\epsilon_i - \epsilon_h}{\epsilon_i + 2\epsilon_h} \mathbf{E}_{\text{loc}} \quad (6)$$

where a is the inclusion radius and E_{loc} is the local field experienced by the inclusion. For sparse, randomly distributed dipoles the local field is given by the Lorenz relation:

$$\mathbf{E}_{\text{loc}} = \mathbf{E}_0 + \frac{4\pi}{3\epsilon_h} \mathbf{P} \quad (7)$$

Simple algebra yields the composite polarization and thus the effective dielectric constant:

$$\frac{\epsilon_{\text{eff}} - \epsilon_h}{\epsilon_{\text{eff}} + 2\epsilon_h} = \beta f \quad \text{where } \beta \equiv \frac{\epsilon_i - \epsilon_h}{\epsilon_i + 2\epsilon_h} \quad (8)$$

Here f represents the volume fill fraction of the inclusion particles.

This expression displays an important feature: for metal inclusion particles, which have a negative real part of the dielectric constant, the real part of the denominator of β may go to zero, implying the existence of a resonance. Maxwell Garnett compared this resonance with the observed colors of several metal-doped glasses. For the samples which met his model criteria, the agreement between the theory and experimental observations was very good. (Several samples had fill fractions so small that the assumption that the interparticle spacing was much smaller than an optical wavelength was violated. For these samples there was still some agreement with the theory, but not as good; they are more accurately described as a collection of scatterers than as an effective medium.) From this work we get an indication that effective medium theory can yield accurate predictions for composite materials. Note also that, although Maxwell Garnett considered

only metallic inclusion particles, the derivation is valid in general, i.e., the constituents may be pure dielectrics as well.

Another important concept evident in the above derivation is that of local fields; the electric field driving the polarization of an inclusion particle is not the same as the macroscopic electric field appearing in Maxwell's equations. Instead it is a local field whose value depends on the polarization of the surrounding medium as well as the applied field. This redistribution of the field between the constituents is the reason that the optical constants of the effective medium are not simply the weighted averages of those of the constituents. Local-field effects play a role in each of the composite geometries to be considered. Their role is even more significant in the nonlinear effective medium theories, since the local-field correction factor appears multiple times in expressions for the nonlinear susceptibilities. (Note: throughout this work, we assume that the nonlinear response of the materials is due to effects which are spatially localized, e.g., due to electronic or molecular orientation effects, so that local fields are important. Thermal nonlinearities are ruled out due to their spatially nonlocal nature.)

The Maxwell Garnett geometry may be generalized by allowing the particles to be nonspherical. Analytic solutions are possible if the inclusions are ellipsoidal (all having the same shape). While numerous orientational correlations between inclusion particles are possible, usually only two extremes are considered: either the inclusions are all oriented the same way or they are randomly oriented. The effective media for these two possibilities are significantly different. For oriented ellipsoids, the composite is anisotropic. Cohen et al.⁶ have modified the Maxwell Garnett derivation by including shape factors describing the ellipsoids and by using an ellipsoidal cavity in determining the local field. The result of their calculation is given by

$$\frac{\epsilon_{\text{eff}} - \epsilon_h}{L\epsilon_{\text{eff}} + (1-L)\epsilon_h} = f \frac{\epsilon_i - \epsilon_h}{L\epsilon_i + (1-L)\epsilon_h} \quad (9)$$

where L is the shape factor. To test their theory, Cohen et al. formed composites by sputtering silica and either silver or gold onto quartz substrates. The composition of the composites formed in this manner varied continuously along the length of the substrate; near the metal target the composite was mostly metallic, whereas near the silica target the composite was mostly silica. For their measurements, they used a thin slit to select various portions of the sample with nearly uniform compositions, but differing fill fractions. By comparing the absorption peak wavelength of the samples versus the volume fill fraction of the metal, they found that the shape of the inclusion particles changed with changing fill fraction. They also verified this fact by electron microscopy. In addition, they found good qualitative agreement between theory and experiment regarding the absorption spectra for various fill fractions.

For randomly oriented ellipsoids the effective medium is isotropic. In this case the result for the linear medium is analogous to the spherical inclusion particle model; however, the shape of the inclusions may have some effect. This difference is significant only when the shape of the particles approaches either extreme (needles

or plates) and the difference between the dielectric constants of the two constituents is large.

The Maxwell Garnett model may be extended to the regime of nonlinear optics. This presents two possibly interesting effects. First the local fields play a much more important role in nonlinear effects; the local-field correction factor, which appears in linear optics to the first power, appears in the third-order susceptibility to the fourth power. Second the resonance appearing in the linear dielectric constant provides the possibility of resonant enhancement of the nonlinearity of the composites. Three different cases must be considered: nonlinear inclusion particles in a linear host, linear inclusion particles in a nonlinear host, and nonlinear inclusion particles in a nonlinear host.

It is rather surprising, considering the age of the Maxwell Garnett theory, that no nonlinear version was developed until the 1980s. The first work done was that by Ricard et al.,⁷ who determined the third-order susceptibility of metal colloids in water. Taking the Maxwell Garnett result to lowest order in the fill fraction:

$$\epsilon_{\text{eff}} \approx \epsilon_h(1 + 3\beta f) \quad (10)$$

a Taylor expansion with respect to a small change in the inclusion dielectric constant was performed:

$$\delta\epsilon_{\text{eff}} = 3\epsilon_h f \frac{\partial\beta}{\partial\epsilon_i} \delta\epsilon_i \quad (11)$$

The change in the inclusion dielectric constant was assumed to be due to a third-order nonlinearity:

$$\delta\epsilon_i = 12\pi\chi_i^{(3)} |E_{\text{loc}}|^2 \quad (12)$$

where E_{loc} is the local-field experienced by the particle. Using the electrostatic electric field experienced by a single sphere in the host material as the local-field, they arrived at the expression

$$\delta\epsilon_{\text{eff}} = f \left(\frac{3\epsilon_h}{\epsilon_i + 2\epsilon_h} \right)^2 \left| \frac{3\epsilon_h}{\epsilon_i + 2\epsilon_h} \right|^2 12\pi\chi_i^{(3)} |E|^2 \quad (13)$$

Note that the local-field correction factor does indeed appear to fourth power in this expression and that it displays the same resonance condition, so the possibility of strong resonant enhancement of $\chi^{(3)}$ exists. Ricard et al. set out to verify this theory by forming composites of silver or gold colloids in water and measuring $\chi^{(3)}$ by degenerate four-wave mixing (DFWM). They selected their wavelengths based on the resonance conditions for the two metals: 532 nm for gold and 396 nm for silver. In both cases they found phase conjugate reflectivities several thousand times stronger on resonance than off resonance. This ratio is consistent with theoretical predictions, which estimate a ratio of the on-resonance to off-resonance reflectivities due to the metal particles on the order of 10^{10} for gold and 10^6 for silver. The smaller measured ratio may be attributed to the additional nonlinear contributions from the host material and the glass windows of the cell.

In subsequent papers Hache et al.^{8,9} considered three possible origins of the nonlinearity of the metal particles: intraband, interband, and hot-electron contributions. The intraband model considered the nonlinearity due to electron transitions within a single conduction band. It was found that for this case $\chi^{(3)}$ is negative

imaginary and scales as the inverse of the particle radius cubed.⁸ The interband model considered the nonlinearity due to electron transitions from the d band to the s conduction band. For this case $\chi^{(3)}$ is negative imaginary and independent of size.⁹ The hot-electron model considered the nonlinearity due to nonequilibrium heating of the conduction band electrons. For this case $\chi^{(3)}$ is positive imaginary and independent of size. The corresponding experiments on gold colloids ranging in size from 28 to 300 Å found little or no size dependence for the nonlinearity. In addition, all of the tensor components of $\chi^{(3)}$ were positive imaginary, except for $\chi_{xyx}^{(3)}$. Thus the hot-electron contribution was dominant, except for the one-tensor component for which it vanishes. In this term the interband contribution dominated.

Three other theoretical formulations of Maxwell Garnett geometry nonlinear composites have been proposed. Agarwal and Dutta Gupta¹⁰ used a T matrix approach to arrive at a general relationship for $\chi^{(3)}$ (and $\chi^{(5)}$ as well) and then determined the forms of the matrices for the case of spherical inclusion particles. Their theory is scalar in nature, i.e. it ignores the tensor nature of $\chi^{(3)}$. The relationship they arrive at is subtly different than that of Ricard et al. in that the local-field correction factor contains the term $\epsilon_{\text{eff}} + 2\epsilon^h$ rather than the term $3\epsilon^h$. The equation of Agarwal and Dutta Gupta is the more accurate one; the expression of Ricard et al. used the low fill fraction approximate equation for the Maxwell Garnett model and approximated the local-field by the single-particle field, ignoring the effects of the other particles on the surrounding linear dielectric constant. However the difference between the two expressions is very small in the low fill fraction limit. For metal colloid composites the fill fraction is typically on the order of 10^{-6} , for which case the effective dielectric constant is very nearly equal to that of the host material.

Sipe and Boyd¹¹ have also developed an effective nonlinear medium theory based on the Maxwell Garnett geometry. Their theory is a fully tensor one which considers the possibility of a nonlinear host as well as nonlinear inclusions. The goal of their work was to determine if enhancement of $\chi^{(3)}$ is possible through the local-field correction factors, even if both constituents are purely dielectric, so no plasma resonance is possible. For the case of nonlinear inclusions in a linear host they found that no enhancement is possible; the relative effective nonlinearity increases monotonically with increasing fill fraction but never goes above unity (see Figure 2a). For the case of linear inclusion particles in a nonlinear host they found that enhancement is possible when the inclusions have a much larger linear index of refraction than the host (see Figure 2b). In this case the dipole field of the inclusions forces the electric field to concentrate in the host, greatly increasing the local-field there. Their results show the relative effective nonlinearity starting at unity at zero fill fraction and increasing monotonically with increasing fill fraction. Thus the larger the fill fraction becomes, the greater the enhancement achieved. This prediction has not yet been tested experimentally, due to the necessity of achieving very large fill fractions, a difficult materials problem. Note that the theory of Sipe and Boyd also covers the case in which both constituents are nonlinear: the result is simply the sum of the results for the

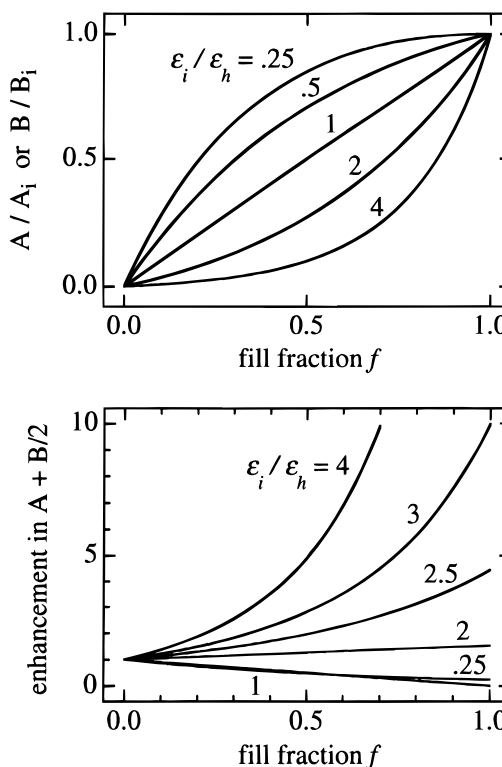


Figure 2. Theoretically predicted, effective nonlinearity of a Maxwell Garnett geometry composite versus the inclusion particle fill fraction. (a, top) Nonlinear inclusion particles in a linear host material. (b, bottom) Linear inclusion particles in a nonlinear host material. [From ref 11.]

two cases of one linear and one nonlinear constituent.

Finally, Stroud and Hui¹² used the concept that the energy dissipated in the composite must be the same as that dissipated by a medium with the same effective dielectric constant to derive an integral expression for the effective medium. They used the low fill fraction approximation in the Maxwell Garnett geometry to arrive at the same relation as Ricard et al.⁷ In a subsequent paper, Zeng et al.¹³ assumed that the electric field was uniform in the nonlinear constituent and performed a Taylor expansion of the linear effective dielectric constant with respect to a perturbation in the value of the constituent dielectric constant. In this case for the Maxwell Garnett geometry they arrived at the more accurate answer for the effective nonlinearity when the inclusions are nonlinear; for a nonlinear host they have a prediction, although it must be recognized that the nonuniform electric field in the host violates their assumptions.

Numerous experiments have been performed on this geometry composite, primarily on metal particles in various hosts. The work of Ricard et al.⁷ and Hache et al.⁹ has already been mentioned. Two points not stated were that they also measured the response time and found it was faster than the laser pulses (~5 ps), so the nonlinearity was electronic in origin. Also they commented on the figure of merit of such composites; since optical loss adversely affects the nonlinear interaction, it is not sufficient to consider only $\chi^{(3)}$. A typical figure of merit for third-order nonlinearities is given by

$$F = \chi^{(3)} / \alpha \tau \quad (14)$$

where α is the linear absorption coefficient and τ is the response time. It can be seen that even though a metal

particle composite has an enhanced value of $\chi^{(3)}$ near resonance, the improvement of the figure of merit is not as large, since the linear absorption also increases sharply near resonance.

Bloemer et al.¹⁴ measured the nonlinearity of gold colloids in water. Using four different inclusion sizes (4.6, 10.9, 15.6, 32.7 nm) they found that $\chi^{(3)}$ is only slightly size dependent, so the hot-electron contribution is most probably dominant. They also compared with theory the shift and broadening of the resonance with increasing inclusion particle size. In some cases they found good agreement, while in others they found significant disagreement. They suggested that probable causes include nonspherical inclusion particle, lattice defects within the inclusions, and contributions from the host matrix. In another experiment Bloemer et al.¹⁵ made of composite of gold in gelatin. They were able to form waveguides and measure $\chi^{(3)}$ by DFWM. They saw no evidence of saturation effects and found fair agreement between a full waveguide based theory and their experiment. La Peruta et al.¹⁶ were also able to form composites of silver particles in a polymer into waveguides. They measured $\chi^{(3)}$ on resonance, finding the expected resonant enhancement. Uchida et al.¹⁷ formed composites consisting of copper or silver doped into glass hosts and found that $\chi^{(3)}$ and α peak at the same wavelength and that their ratio is approximately constant as a function of fill fraction. (Thus, increasing the volume fraction of the metal to increase the nonlinear response will not improve the material performance, since the figure of merit remains constant.) They also found evidence of two response times: the faster one (~ 12 ps) was attributed to the electronic response, while the slower one (~ 200 ps) was attributed to thermal effects.

The group including Magruder, Haglund, Yang, and several others have performed a number of experiments on composites formed by ion implantation of metals into glass.^{18–24} The composites formed in this manner are thin layers (~ 150 nm) at the surface of the glass. In one experiment on copper-doped glasses¹⁹ they used forward DFWM to determine the $xyxy$ component of $\chi^{(3)}$ (eliminating the possibility of either thermal or hot-electron contributions). They found a particle size dependence to $\chi^{(3)}$ that went nearly as the inverse of the radius cubed, implying that the intraband contribution was important for these composites. This result is different from that of Hache et al.,⁹ who found that the hot-electron contribution dominated for gold particles. This may be explained by noting that the intraband and interband terms are wavelength dependent, so the quantum size enhancement may hold at one wavelength, but not another. In another experiment Magruder et al.²⁰ doped both silver and copper into glass and found evidence that the two metals interact and that the silver enhances the response of the copper near resonance (see Figure 3 and Table 1).

Numerous theories and experiments have also addressed composites consisting of semiconductor nanocrystallite inclusions dispersed in a host. In determining the linear optical absorption of such particles Efros and Efros²⁵ divided the problem into three regimes based on the radius of the crystallites, a , versus the Bohr radii of the electrons and holes, a_e and a_h . In the strong confinement regime ($a \ll a_e$ and $a \ll a_h$) the absorption spectrum was determined to be discrete lines

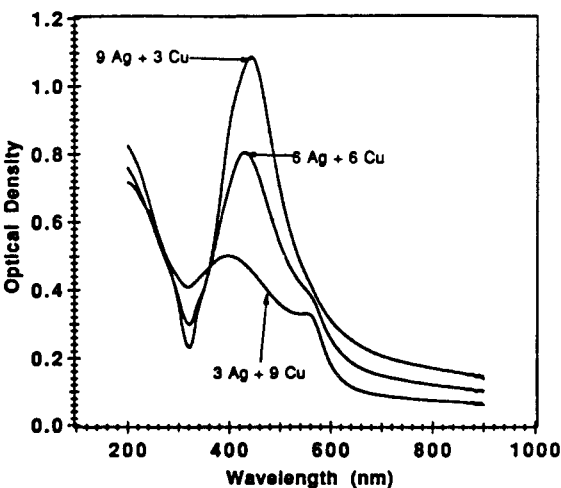


Figure 3. Optical density of copper and silver co-doped into silica glass. The presence of the silver affects the absorption at the copper particle resonance. [From ref 20.]

Table 1. Linear and Nonlinear Optical Coefficients Measured at 570 nm^a

| sample | α (cm $^{-1}$) | n_2 (cm 2 /W) | β (cm/W) |
|------------|------------------------|----------------------|-----------------------|
| 9Ag to 3Cu | 5.9×10^4 | 1.0×10^{-9} | 3.8×10^{-5} |
| 6Ag to 6Cu | 5.4×10^4 | 1.3×10^{-9} | -0.9×10^{-5} |
| 3Ag to 9Cu | 4.6×10^4 | 1.6×10^{-9} | -1.4×10^{-5} |

^a α , absorption coefficient; n_2 , index of refraction; β , two-photo absorption coefficient.

which were blue-shifted with respect to the bulk band-gap wavelength. The magnitude of the shift was influenced by the electron mass. In the intermediate confinement regime ($a_h < a < a_e$) this same blue-shift was found. In the weak confinement regime ($a_h \ll a$ and $a_e \ll a$) an energy shift was also present, but it was determined by the total exciton mass.

The first measurement of the nonlinear susceptibility of a semiconductor nanocrystallite composite was performed by Jain and Lind.²⁶ Using standard Corning and Schott glass filters, which were glasses doped with CdSSe particles, they made DFWM measurements to determine the magnitude of $\chi^{(3)}$ and the response time. Their results showed large nonlinearities ($\sim 10^{-8}$ esu) and subnanosecond recovery times. This work encouraged many groups to perform measurements on similar samples.^{27–40} Enhanced nonlinearity due to quantum confinement,³⁷ femtosecond response times,³⁵ saturable absorption,³¹ nonlinear susceptibilities around 10^{-4} at low temperatures,³³ and alteration of saturation intensity with crystal size³⁸ all have been observed. We will not go into the details of these works, since, as Ricard et al.³⁶ pointed out, the local-field effects (and thus the composite nature of these materials) play almost no role in the optical properties due to the low fill fractions and lack of resonance effects. The interested reader is referred to the references already cited as well as the review papers by Brus,⁴¹ Reisfeld,⁴² and Alivisatos.⁴³

Modifications of the Maxwell Garnett geometry may also be considered in the nonlinear regime. For the case of ellipsoidal inclusions Haus et al.⁴⁴ have performed a theoretical calculation of the effective third-order nonlinearity. Using a self-consistency approach, they found analytic expressions for effective nonlinearity for spheroidal inclusion particles which were either completely oriented or randomly oriented. For the completely oriented particles they found that, even though the constituent nonlinearities were assumed to be third-

Table 2. Composite Model Calculations for the Electrostrictive Mechanism in a Polystyrene Composite^a

| model | | | | | conjugate signal $\chi_{\text{eff}}^{(3)}$ (esu) | absorption | |
|-------|--------|---------|-------------------|------------------|--|------------------------------|--------------------|
| core | shell | medium | r_1/r_2 | λ (nm) | | γ (cm ⁻¹) | η (esu cm) |
| PS | | water | 1.0 | 500 ^b | 3×10^{-6} | 30 ^c | 3×10^{-6} |
| Au | PS | water | 0.5 | 500 | 6×10^{-5} | 1×10^3 | 2×10^{-6} |
| PS | Au | water | 0.6 | 500 | 2×10^{-3} | 2×10^4 | 3×10^{-6} |
| PS | Au | water | 0.8 | 628 | 9×10^{-3} | 3×10^4 | 9×10^{-6} |
| PS | Au | water | 0.9 | 942 | 2×10^{-2} | 3×10^4 | 2×10^{-5} |
| Al | PS | water | 0.5 | 500 ^b | 9×10^{-5} | 1×10^2 | 3×10^{-5} |
| PS | Al | water | 0.92 ^d | 500 | 1×10^{-2} | 8×10^4 | 4×10^{-6} |
| Al | silica | organic | 0.5 ^e | 200 | 2×10^{-5} | 1×10^4 | 6×10^{-8} |

^a $2r_2 = 100$ nm, $\rho = 1\%$. For (3.7°) coarse grating $\tau = 33$ ms; for (176°) fine grating $\tau = 50$ μ s. For $r_2 = 100$ nm, all electrostrictive $\chi_{\text{eff}}^{(3)}$ are increased by 10^3 , and both τ 's are increased by 10. ^b Nonresonant. ^c γ_s dominant; otherwise γ_m dominates γ . ^d Particle, $2r_2 = 50$ nm. ^e Particle, $2r_2 = 10$ nm.

order, the composite had nonlinearity to all orders and bistability was possible. In another paper Haus et al.⁴⁵ investigated the behavior of such spheroidal composites. They found that the position of the resonance can be controlled by the particle shape and that $\chi^{(3)}$ displays two resonances, even if the particles are randomly oriented. They performed DFWM experiments on gold-doped glass composites (Schott RG6 filter) and found two indications of spheroidal particles. First, the linear absorption peak was broader than that predicted for spherical inclusion particles (see Figure 4a). A better match to theory was obtained when they assumed some spherical inclusions (17%) and some prolate spheroidal inclusions (83%). Second, a plot of the phase conjugate reflectivity versus wavelength displayed two peaks for two of their samples (see Figure 4b). The paper also considers theoretically the possibility of bistability in these materials. They found that intrinsic bistability is possible and the particle shape affects the turning point.

Another modification of the basic MG geometry is to form inclusion particles consisting of a spherical core material surrounded by a concentric spherical shell. For such composites it is possible to use the concentration of the electric field in the vicinity of the core, as well as that inside the core, for enhancement of the overall nonlinearity. Neeves and Birnboim^{46,47} have analyzed such structures and determined their effective third-order susceptibilities for both electrostrictive and electronic contributions. Using a metallic core to strongly increase the field in the shell (or a metallic shell to increase the field in the core), they found it was possible to achieve a resonant enhancement of $\chi^{(3)}$ by a factor of 10^4 and a corresponding increase in the figure of merit by a factor of between 10 and 10^3 (see Figure 5 and Table 2). Thus the absorption of these composites does not increase as rapidly as the nonlinearity near resonance. In their paper utilizing numerical methods, Zhang and Stroud⁴⁸ considered particles consisting of a gold core with an unspecified nonlinear material for the shell. They also found that enhancements on the order of 100 were possible. In addition, they commented that there is an optimal shell thickness, which depends on the parameters of the materials used. Wang and Li⁴⁹ performed a similar analysis, using a T matrix approach to determine the effective value of $\chi^{(3)}$, arriving at similar results.

Particles matching the description of this model have been constructed by Zhou et al.⁵⁰ by reducing the bonds on the surface of a gold-sulfide particle to form a gold coating. They measured the linear absorption properties of their samples, finding a red shift of the peak of

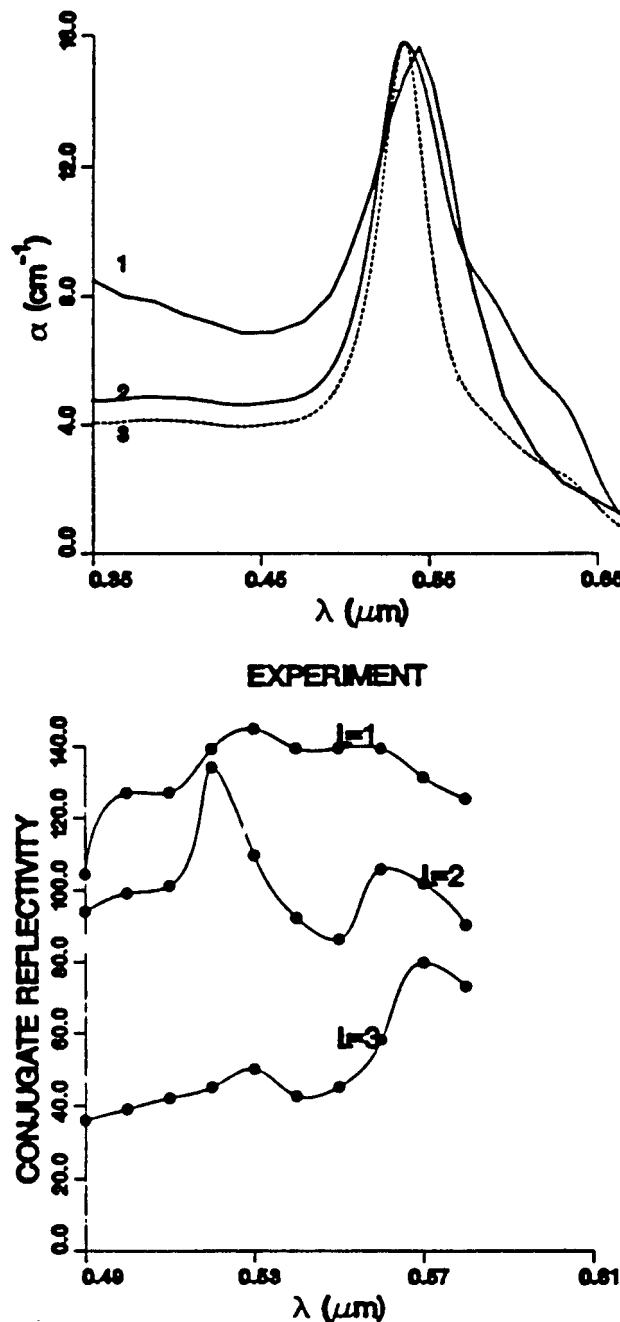


Figure 4. (a, top) Linear absorption of Schott RG6 filter glass. Line 1 is the experimental data and lines 2 and 3 are the theoretical predictions for part spherical and part spheroidal inclusions and for all spherical inclusions. (b, bottom) Phase conjugate reflectivity plotted as a function of wavelength for three RG6 samples. The data display two peaks, indicating two distinct resonance frequencies. [From ref 45.]

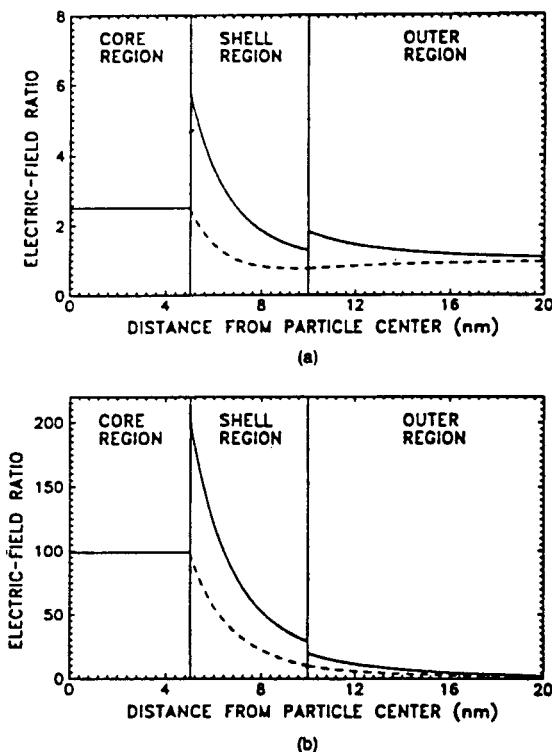


Figure 5. Electric field distribution in the vicinity of a coated inclusion particle. The solid lines represent the field component parallel to the applied field \mathbf{E}_0 , while the dashed lines represent the component perpendicular to \mathbf{E}_0 . Note the large field in the shell region. (a) Gold core. (b) Aluminum core. [From ref 46.]

the plasmon resonance with increasing particle size, in agreement with theoretical predictions.

Kalyaniwala et al.⁵¹ extended the analysis to the case of confocal ellipsoids, specifically considering the case of a semiconductor core surrounded by a metal shell. They used the parameters of CuCl, CdS, and GaAs for the semiconductor material and silver for the metal and found the existence of intrinsic bistability in such composites, with the potential for much lower thresholds than for composites of pure metals. They also analyzed the propagation of a light wave through the composite. They found that, due to the loss, a wave with sufficient energy to induce the higher bistable field in the cores will only do so in the first micrometer length. After this the intensity has decreased to a point where the wave is on the lower part of the bistable curve. Therefore there is a limitation to the practical interaction length.

To summarize the Maxwell Garnett composites, modern theories allow one to determine the effective linear and nonlinear susceptibilities for a composite consisting of spherical (or ellipsoidal) inclusions randomly dispersed in a host material. The results display resonant enhancement when the inclusions are metallic and the host dielectric. In addition local-field effects may lead to enhancement of the overall nonlinearity even off resonance in certain special cases. These same local-field effects may lead to intrinsic bistability in the composites.

3. Bruggeman Geometry

The principle difficulty with the Maxwell Garnett model is that it treats the constituents asymmetrically; one component constitutes inclusion particles while the other constitutes the host. Thus the model only applies

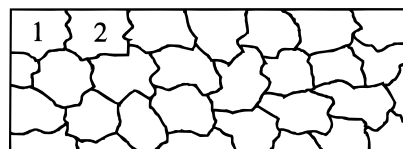


Figure 6. Bruggeman (interspersed) composite geometry.

to composites in which one component occupies a small volume fraction of the total material.

Another common composite model, often called the effective medium theory (EMT) or the Bruggeman theory, avoids this problem by treating the constituents symmetrically. The model assumes that grains of two or more materials are randomly interspersed (see Figure 6). It was first proposed and analyzed by Bruggeman⁵² in 1935. Since his paper is written in German, we look to more recent analyses, e.g., those by Landauer,⁵³ which arrive at the same result, albeit with respect to the analogous parameter of effective conductivity, and by Stroud.⁵⁴ To analyze such a composite, one considers a single grain within the whole. This grain will be surrounded by grains of each type of constituent material, including its own type. We thus make the approximation that the grain is surrounded by a material of uniform dielectric constant given by that of the effective medium. If we take the grain to be spherical, we may solve for the internal electric field due to a uniform applied field E_0 :

$$\mathbf{E}_i = \frac{3\epsilon_{\text{eff}}}{\epsilon_i + 2\epsilon_{\text{eff}}} \mathbf{E}_0 \quad (15)$$

which leads to a displacement field of the form

$$\mathbf{D}_i = \frac{3\epsilon_{\text{eff}}}{\epsilon_i + 2\epsilon_{\text{eff}}} \mathbf{E}_0 \quad (16)$$

Treating the grains of the other constituents in the same manner, we may determine the average displacement field of the composite by taking the weighted sum of the fields of the individual grains:

$$\mathbf{D} = f_1 \mathbf{D}_1 + f_2 \mathbf{D}_2 \quad (17)$$

This field is simply related to the effective dielectric constant:

$$\epsilon_{\text{eff}} \mathbf{E}_0 = \mathbf{D} \quad (18)$$

Thus we arrive at the relation for the linear effective medium:

$$0 = f_1 \frac{\epsilon_1 - \epsilon_{\text{eff}}}{\epsilon_1 + 2\epsilon_{\text{eff}}} + f_2 \frac{\epsilon_2 - \epsilon_{\text{eff}}}{\epsilon_2 + 2\epsilon_{\text{eff}}} \quad (19)$$

It is readily apparent that this formula is symmetric with respect to the constituents. This theory will be applicable for materials in which all components occupy large volume fractions of the whole.

There is an important feature of composites predicted by this model. As the volume fraction of one constituent increases from very small values, there will come a point at which the grains begin to join and form continuous threads throughout the composite. At this percolation threshold the properties of the composite (especially the conductivity of a metal/insulator composite) may change significantly. For a metal/insulator composite the per-

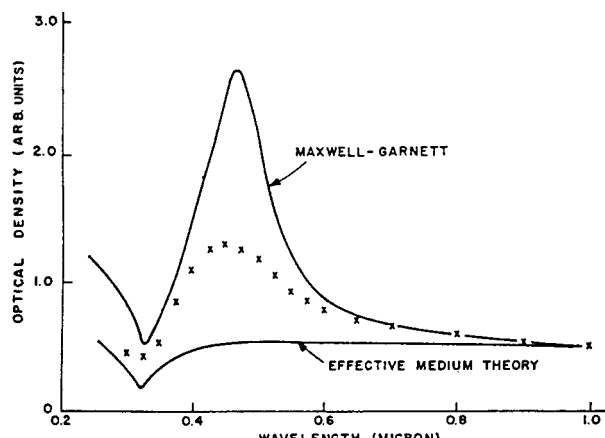


Figure 7. Comparison of the measured optical density of a silver in silica glass composite containing 39% silver (crosses) with the predictions of the Maxwell Garnett and the effective medium theories. The Maxwell Garnett model overestimates the strength of the resonance, while the Bruggeman model does not predict the resonance. [From ref 56.]

colation threshold is the point at which the conductivity becomes nonzero, i.e., the composite appears as a metal rather than an insulator. These changes are correctly accounted for by the Bruggeman theory but not by the Maxwell Garnett theory. Experimentally, the percolation threshold has been detected in actual composites, although at volume fractions slightly larger than the theory indicates.⁵⁵

Another difference between the predictions of the Bruggeman and the Maxwell Garnett models appears in the behavior near the surface plasmon resonance of metal particles in a dielectric. At very low volume fractions of the metallic constituent, the predictions of the two models are virtually identical. However, as the volume fraction increases, the Maxwell Garnett model continues to predict a sharp resonance, whereas the Bruggeman model predicts a broadening and weakening of the resonance (see Figure 7⁵⁶). This fact has led Sheng⁵⁵ to suggest a modification which combines the two models. For a two component composite, instead of a grain consisting of a single material, Sheng considers a grain consisting of a core of one material with a shell of the other material. The dimensions of the core and shell are such that the volume fraction of each material is the same as that in the composite as a whole. Sheng determined the probability of a core of material 1 with a shell of material 2 and vice versa and then proceeded with an analysis similar to that described above. Thus the symmetric treatment of the constituents is preserved, while the use of the relative probabilities of the two core/shell combinations results in accurate predictions in the low volume fraction limit, i.e., the dielectric anomaly is also preserved. He compared the predictions to several actual composites; his results are shown in Figure 8. We see that the model agrees well with the data for each volume fraction.

Experimental work has called into question the validity of the Bruggeman model for predicting the functional dependence of the linear effective dielectric constant on fill fraction in metal/insulator composites. In an experiment performed by Grannan et al.,⁵⁷ composites of silver particles embedded in a KCl host were manufactured at various fill fractions below the percolation threshold and the effective dielectric constant was measured. The authors noted that if one used a modified form of the

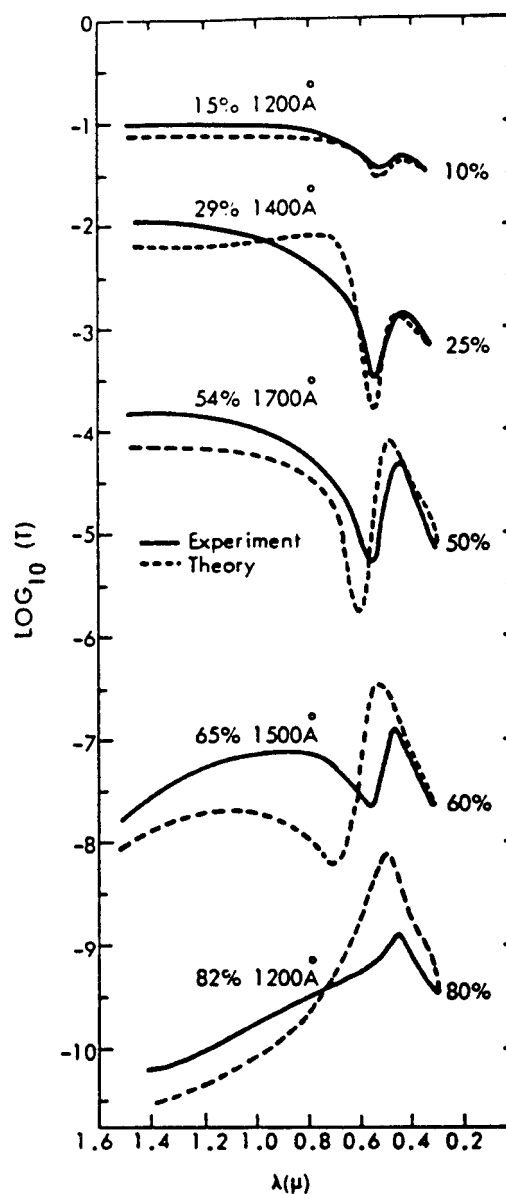


Figure 8. Comparison of the modified theory by Sheng⁵⁵ with experimental data for gold/silica glass composites. (The curves are displaced with respect to each other for the sake of clarity.) [From ref 55.]

fill fraction defined as

$$f^* = (f_c - f)/f_c \quad (20)$$

where f_c is the percolation threshold, that the dielectric constant followed the functional form:

$$\epsilon_{\text{eff}} = A/(f^*)^s \quad (21)$$

where the exponent s was found to equal approximately 0.73. For their experiments, Grannan et al. measured a percolation threshold of around 20%. Berthier et al.⁵⁸ subsequently noted that the Bruggeman theory predicts approximately the following form for the effective medium:

$$\epsilon_{\text{eff}} = A/f^* \quad (22)$$

Thus the predicted exponent is inaccurate. In this case it is important also to note that the critical fill fraction

quoted by Grannan et al. is significantly smaller than that predicted by the Bruggeman theory (33.3%). This difference demonstrates that the Bruggeman model does not accurately describe these real composites. This is not truly surprising, since the assumptions underlying the derivation, namely, spherical grains with uniform internal electric fields, are too strong to be realistic. Thus the Bruggeman theory may be more useful for its qualitative predictions and the intuition regarding composite behavior which they provide than for quantitative analysis.

Theories regarding the nonlinear properties of Bruggeman geometry composites typically use even stronger simplifying assumptions. If one followed the derivation of Landauer, one would need to determine the polarization of a spherical particle with one nonlinear susceptibility embedded in a host with another nonlinear susceptibility. This proves to be a difficult analysis. It is thus necessary to simplify the problem. For example, Zeng et al.¹³ assumed that the electric field is still uniform within each grain and that the nonlinearity represented a perturbation to the dielectric constant of each constituent material. They thus were able to perform a Taylor expansion of the effective dielectric constant with respect to small changes in each of the constituent dielectric constants. They used the local-field from the linear field calculation to determine to lowest order the magnitude of the perturbations. Their result was

$$\chi_{\text{eff}}^{(3)} = \frac{\chi_1^{(3)}}{f_1} \left(\frac{\partial \epsilon_e}{\partial \epsilon_1} \right)_0 \frac{\partial \epsilon_e}{\partial \epsilon_1} + \frac{\chi_2^{(3)}}{f_2} \left(\frac{\partial \epsilon_e}{\partial \epsilon_2} \right)_0 \frac{\partial \epsilon_e}{\partial \epsilon_2} \quad (23)$$

where the derivatives are determined from the expression for the linear effective dielectric constant:

$$0 = f_1 \frac{\epsilon_1 - \epsilon_{\text{eff}}}{\epsilon_1 + 2\epsilon_{\text{eff}}} + f_2 \frac{\epsilon_2 - \epsilon_{\text{eff}}}{\epsilon_2 + 2\epsilon_{\text{eff}}} \quad (24)$$

Another approach to nonlinear EMT theories is to use numerical methods. In two papers Zhang and Stroud^{48,59} compared results of numerical calculations on random three-dimensional binary composites with the predictions of the linear and nonlinear EMT. (They actually considered the analogous property of conductivity, not the dielectric constant.) They analyzed composites of two different conductors at zero frequency and composites of a conductor and an insulator at finite frequencies. Four different fill fractions were considered: 1%, 24.92% (the percolation threshold), 50%, and 90%. In all cases they found good quantitative agreement between simulation and theory in the linear limit (see Figure 9). However, there was not good agreement between simulation and theory for the nonlinear properties (see Figure 10). For the two conductor composites, the EMT overestimated the enhancement of the nonlinearity of the poor conductor by a significant amount. For the insulator/conductor composites, plots of the nonlinear susceptibility versus frequency show interesting features and large enhancements in the simulations which do not appear in the analytic theory. In their papers Zhang and Stroud hypothesize that the differences are due to the critical dependence of the nonlinear susceptibility on the composite microstructure: there exists the possibility of strong localized surface plasmon resonances. To demonstrate this, in ref 59 they added

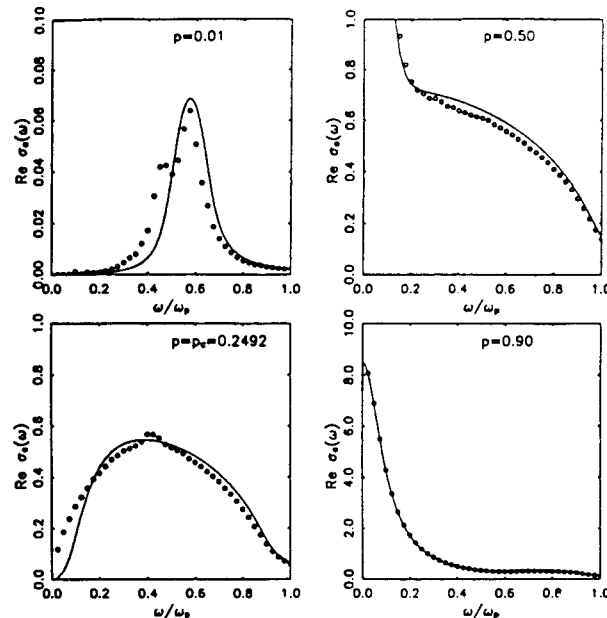


Figure 9. Comparison of the predictions of the linear effective medium theory (solid lines) and numerical simulations (circles) for the effective electrical conductivity of a metal/insulator composite. [From ref 48.]

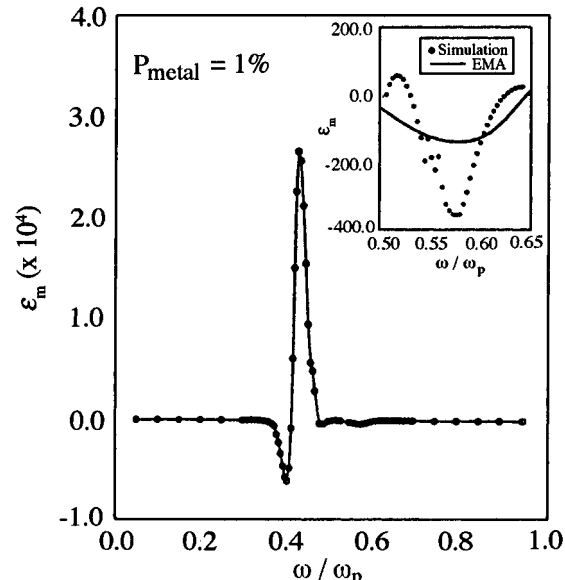


Figure 10. Comparison of the predictions of the effective nonlinear electrical conductivity of a metal/insulator composite. The differences between the two results, shown in the inset, indicate the inaccuracy of the nonlinear effective medium theory. [From ref 59.]

correction terms to the effective dielectric constant consisting of weak surface plasmon resonant terms. These terms had little impact on the linear effective dielectric constant but significantly altered the calculated nonlinear susceptibility. In this way they were able to produce a prediction which had qualitatively similar enhancement peaks as the numerical simulations.

4. Layered Geometry

Another common composite geometry is that of alternating layers of two or more materials (see Figure 11). Such a composite is not isotropic: the optical properties for electric fields polarized parallel to the layers will

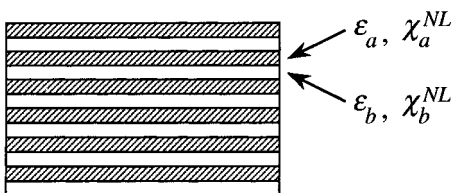


Figure 11. Layered composite geometry.

typically be different than those for electric fields polarized perpendicular to the layers. Thus the composite is uniaxial with its optic axis normal to the layers.

To develop an effective medium theory, one must simply assume that each layer is much thinner than an optical wavelength. Spatial averaging of the mesoscopic fields to arrive at the macroscopic parameters is straightforward due to the simplicity of the geometry. Several analyses for the linear^{13,60,61} and nonlinear^{13,61} optical properties have been carried out. For electric fields parallel to the layers, the field is continuous across the boundaries, so the effective linear dielectric constant and nonlinear susceptibilities are merely the weighted averages of those of the constituents:

$$\epsilon_{\parallel} = f_1 \epsilon_1 + f_2 \epsilon_2 \quad (25a)$$

$$\chi_{\parallel}^{NL} = f_1 \chi_1 + f_2 \chi_2 \quad (25b)$$

When the electric field is polarized perpendicular to the layers more interesting effects occur. In this case the displacement field is continuous across the boundaries, so the electric field is nonuniformly distributed between the layers. Thus local-field effects play a role. It has been shown^{13,60,61} for the linear medium that the effective dielectric constant is given by

$$\frac{1}{\epsilon_{\perp}} = \frac{f_1}{\epsilon_1} + \frac{f_2}{\epsilon_2} \quad (26)$$

Expressions for the effective nonlinear susceptibilities depend on the specific nonlinear process considered. For the nonlinear refractive index Boyd and Sipe⁶¹ found the following expression for $\chi^{(3)}$:

$$\begin{aligned} \chi_{eff}^{(3)}(\omega = \omega + \omega - \omega) = & f_a \left(\frac{\epsilon_{\perp}(\omega)}{\epsilon_a(\omega)} \right)^2 \left| \frac{\epsilon_{\perp}(\omega)}{\epsilon_a(\omega)} \right|^2 \chi_a^{(3)} + \\ & f_b \left(\frac{\epsilon_{\perp}(\omega)}{\epsilon_b(\omega)} \right)^2 \left| \frac{\epsilon_{\perp}(\omega)}{\epsilon_b(\omega)} \right|^2 \chi_b^{(3)} \end{aligned} \quad (27)$$

Notice that the local-field correction factor is the ratio of the effective linear dielectric constant to that of the constituents. For one constituent this factor must be larger than unity, while for the other it is less than unity (unless it equals unity for both, the trivial case). Thus if the constituent for which the factor is greater than unity is the strongly nonlinear one, enhancement is possible. Boyd and Sipe have plotted the behavior of the effective nonlinearity versus volume fill fraction of one constituent using the ratio of the linear dielectric constants of the constituents as a parameter (see Figure 12). It is readily apparent that for large ratios enhancement of up to an order of magnitude is obtainable. Note that the fill fraction for maximum enhancement is approximately 80% for the linear constituent. This indicates the importance of the local-field factor; a composite in which the nonlinear component constitutes

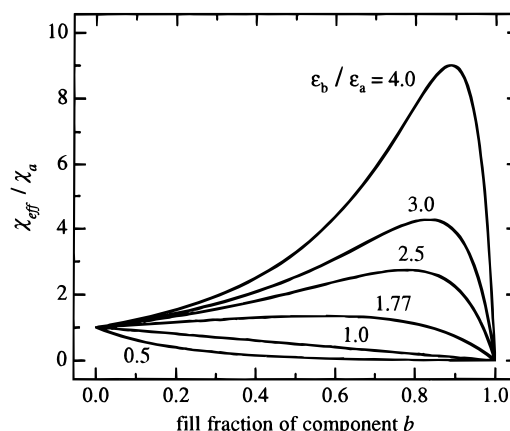


Figure 12. Effective nonlinear refractive index of a layered composite assuming that only constituent *a* is nonlinear. Note that if the linear dielectric constants of the two constituents differ by a factor of 4, the nonlinear response can be enhanced by a factor of 9. [From ref 61.]

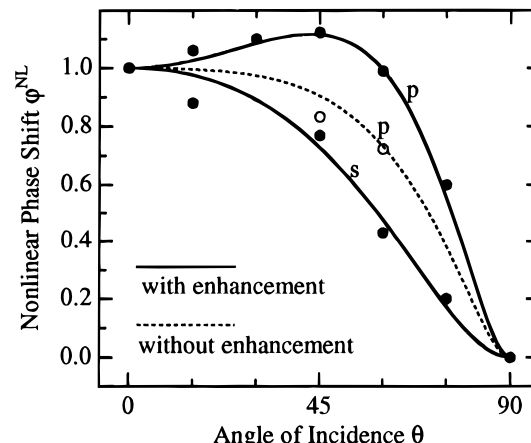


Figure 13. Measured nonlinear response of the PBZT/titanium dioxide composite for both *s*- and *p*-polarized light (solid circles) and of pure PBZT for *p*-polarized light (open circles). The solid curves show the theoretical predictions and the dashed curve shows the expected behavior if there was no local field enhancement of $\chi^{(3)}$. [From ref 62.]

only 20% of the volume may, through local-field effects, have a nonlinearity enhanced by a factor of nearly 10 over that of the pure nonlinear material.

Fischer et al.⁶² have performed experiments to verify some of the predictions of this theory. They constructed a composite consisting of alternating layers of titanium dioxide and the conjugated polymer poly(*p*-phenylenebenzobisthiazole) (PBZT) by means of spin casting. The layer thicknesses of the TiO₂ and the PBZT were 500 and 400 Å, respectively, which yielded nearly the ideal fill fraction for enhancement given the linear refractive indexes of the constituents. For their composite the expected enhancement was 35%. The nonlinearity was measured using a z-scan setup⁶³ with the sample placed at various angles with respect to the beam axis (thus achieving a component of the electric field normal to the layers). Analysis of the data was accomplished by determining the nonlinear phase shift experienced by a plane wave propagating through a uniaxial material described by the composite effective material parameters.⁶⁴ The results of their measurements along with their theoretical predictions are shown in Figure 13. It is evident that the theory, which includes the effective medium predictions, gives a good description of the experiment. Also note that the open

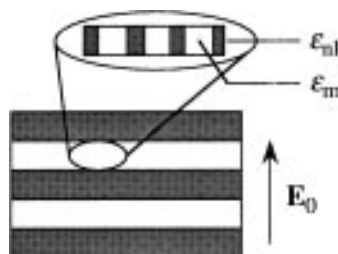


Figure 14. Three-component layered composite.

circles on the graph, which represent z-scan measurements of the pure polymer, fall on the dotted line representing the theoretical prediction for p-polarized light falling on an isotropic material. This indicates that the source of the enhancement is in fact the local-field effects and not an anisotropy in the constituent.

Bergman et al.⁶⁵ have considered the possibility of bistability in such composites when one constituent is an optically linear metal and the other constituent is an optically nonlinear dielectric. They derived a cubic equation for the square of the electric field inside the dielectric and determined conditions for there to exist three real roots. However, due to the difficulty of the analysis they did not show which of the roots was stable. Instead they hypothesized that only two would be stable, i.e., bistability exists in these composites.

Levy et al.⁶⁶ added a twist to such composites: they considered the possibility of using a layered composite as one constituent of a layered composite (see Figure 14). Using the application example of electric-field-induced tuning of the transmission of a thin film, they compared the efficiency of a standard two component composite with their three-component composite. They found that it was possible to tune between 0% and 80% transmission and that the three-constituent composite required a much smaller applied field to accomplish this: on the order of 10^4 V/cm versus 10^5 V/cm.

The group of Zhou, Sheng, Chen, and Chui^{60,67} have suggested using layered composites in a novel manner. They have shown that infrared absorption peaks of an array of rods of metal/insulator layered composites may be tuned by adjusting the array geometry. They performed their calculations in two manners: numerically from first principles and numerically using the effective medium parameters for the rods. Their results demonstrated that as long as the rods are wide enough that edge effects do not dominate, the effective medium approximation gives accurate results and is far less computationally intensive than the full first principles analysis.

5. Fractal Structures

A different type of optical composite is formed when one of the constituents forms fractal structures within the whole. For example, one constituent could consist of metal spheres which clump together forming aggregates with fractal dimension. The manner in which the clusters form will affect their fractal dimension, which in turn affects the optical properties. The problem is thus very involved.

The potential for strong local-field effects in fractal structures is great due to their geometry. Fractals do not possess translational symmetry (instead they possess scale symmetry) so they cannot propagate pure traveling waves. Thus the field excitations are localized,

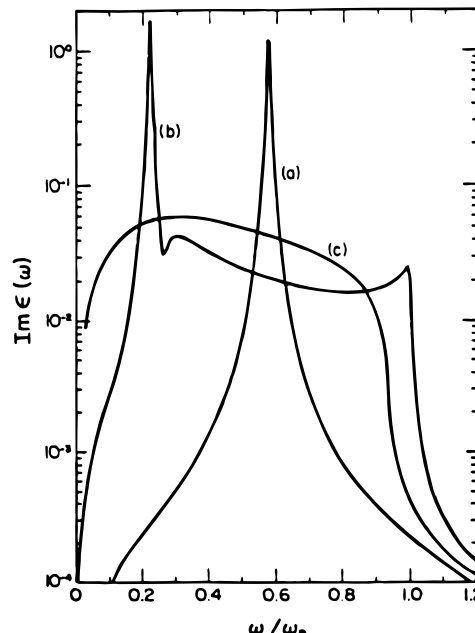


Figure 15. Imaginary part of the effective linear dielectric constant for metal inclusions in a host material. (a) Maxwell Garnett model prediction. (b) Effective medium approximation with fractal clustering of the inclusion particles. (c) Effective medium approximation with nonfractal clustering of the inclusion particles. [From ref 70.]

which may lead to (subwavelength) regions of enhanced absorption, etc.⁶⁸

When considering the linear optical properties of fractal composites, most of the workers are specifically concerned with determining the scattering and absorption cross sections.^{68–72} One of the early analyses of this sort was performed by Berry and Percival,⁶⁹ who were actually interested in the optical properties of smoke. Considering fractal arrays of spherical particles, they found that there are qualitative differences in the optical properties for fractal dimensions less than and greater than 2 (i.e., whether or not the fractal occupies area). For fractal dimensions less than 2 they found that multiple scattering is not significant and the absorption cross section simply equals N times that of a single sphere, where N is the number of monomers comprising the fractal. The scattering cross section was found to increase with the number of monomers until the size of the fractal becomes comparable to an optical wavelength and saturation occurs.

Hui and Stroud⁷⁰ analyzed the linear properties of fractal composites using a three-dimensional differential effective medium approach on self-similar clusters. Their theory assumed knowledge of how fill fraction changes with increase in cluster size and used Mie theory to arrive at the composite extinction coefficient. They found that the electric dipole absorption displays a large increase over that of the monomer. The predictions include a broadening and a red-shift of the absorption (see Figure 15). They note that experiments performed on fractal type structures have seen the resonance broadening but not the red-shift. They hypothesized that this is due to a lack of large clusters in those composites.

The approach of Shalaev and Stockman⁷¹ to fractal composites used a binary approximation, which assumes that one need only consider dipole-dipole coupling of the monomer to its nearest neighbor. The effects of the

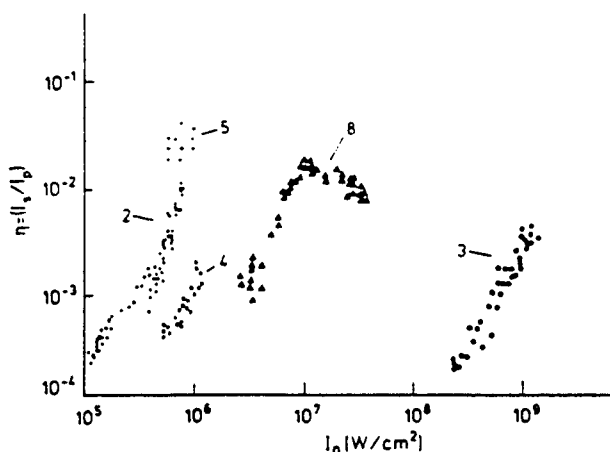


Figure 16. Efficiency of DFWM as a function of the pump irradiance. Data points labeled 2, 4, and 5 represent aggregated inclusions, while data labeled 3 represents stabilized monomers. [From ref 76.]

other monomers was accounted for using a modified Lorenz local field. The results predict a broadening and shift of resonance, as did those of Hui and Stroud. In addition, they predict the possibility of giant Raman scattering: an impurity which causes Raman scattering may see a local-field much larger than the applied electric field due to its neighboring monomer.

Markel et al.^{68,72} have performed more rigorous analyses based on the exact properties of dipole polarizability and on the assumption of scaling for dipole eigenstates of fractals. They found some results in agreement with simpler theories: the width of the absorption peak of the fractal is much greater than that of the monomer. However, they found that the binary approximation may not give accurate predictions for the height at the peak of the absorption. In addition they found that for clusters of more than 15 monomers, the dependence of the polarizability on N had practically leveled off.

Determination of the nonlinear optical properties of fractal composites is an even more difficult task. Butenko et al.^{73,74} used the binary approximation to determine enhancement factors for various n th-order nonlinear processes arising from the nonlinearities of impurities linked to the fractal. (Their definition of the enhancement factor was the ratio of the n th power of the field intensity at a bound impurity to that of the unbound impurities.) They found that this factor can be very large due to the strong localized fields within the fractal structure. Their predictions were verified by Rautian et al.⁷⁵ and Butenko et al.⁷⁶ using fractal clusters of silver in solution. In ref 76 a degenerate four-wave mixing experiment (using a frequency-doubled Q-switched Nd:YAG laser) found that the aggregate samples displayed the same return as the nonaggregate sample when the input irradiance was a factor to 10^3 lower (see Figure 16). Thus the nonlinear efficiency was greater by a factor of 10^6 .

Shalaev et al.^{77,78} used a scale-invariant theory to determine forms for this gain factor. They found that for degenerate four-wave mixing the factor varies as $|\text{Im } \chi_0|^{-6}$. For metallic spheres they calculated this value to be on the order of 10^6 , in agreement with the above results. A set of works by this group of authors^{79–82} finds similar results for other sources of the nonlinearity, such as Raman scattering and the nonlinear refractive index.

Yu et al.^{83,84} have also analyzed the nonlinear behavior of fractal clusters in a host assuming that the fractals occupy a small volume fraction and that the nonlinearity is weak (permitting a perturbative approach). Considering nonlinear conductivity (which is analogous to nonlinear susceptibility), they compared the predictions of a differential effective medium theory with numerical simulations. Their results show good agreement between the two approaches, which indicated the possibility of a large enhancement of the effective nonlinearity when the fractal cluster is nonlinear and the host is the better conductor. Comparing the result for these materials with the predictions of the Maxwell Garnett theory (i.e., unclustered inclusions), Yu⁸⁴ found that the ratio of the imaginary part of the nonlinearities scaled as $f^{-5/2}$, where f is the volume fraction occupied by the fractal. Since this ratio may be very large, the clustering of the inclusion particles has greatly enhanced the nonlinear response of the composite.

Choy and Yu^{85,86} have extended the analysis to strongly nonlinear materials. They again have compared the results of the differential effective medium theory with numerical simulations, finding good agreement. They have determined a scaling law for the effective nonlinear response and found that it is different for superconductor/conductor composites and for conductor/insulator composites.

This review of the optical properties of fractal composites has been by necessity very brief. For a more thorough coverage, the reader is referred to the review article by Clerc et al.⁸⁷

6. Conclusion

In this paper we have provided a brief review of the optical properties of composite materials. The discussion was divided into categories defined by the composite geometries: the Maxwell Garnett, which consists of spherical inclusions randomly dispersed in a host; the Bruggeman, which consists of two (or more) randomly interspersed materials; the layered geometry; and fractal structures. In all cases the interest lies in accurately predicting the linear and nonlinear optical constants and especially to find cases when these properties are enhanced with respect to those of the constituents. As has been shown, the successes of these theories is mixed. For example, the Maxwell Garnett model correctly predicts the surface plasmon resonance of metallic inclusions but can overestimate the strength of the effect; the Bruggeman model predicts a percolation threshold, but due in part to the correlations between neighboring particles, the percolation threshold of real composites typically occurs at lower volume fill fractions than the theory suggests. Still, if one keeps in mind that these models are only approximations to actual composites, these theories can provide one with intuition about the causes for the composite properties and simple relationships with which to predict approximately their behavior.

Acknowledgment. We gratefully acknowledge S. A. Jenekhe, J. E. Sipe, and G. L. Fischer for helpful discussions. This work was supported by the U.S. National Science Foundation, by the U.S. Army Research Office, and by the New York State Science and Technology Foundation.

References

- (1) Maxwell Garnett, J. C. *Philos. Trans. R. Soc. London* **1904**, *203*, 385; **1906**, *205*, 237.
- (2) Brown, W. F. *J. Chem. Phys.* **1955**, *23*, 1514.
- (3) See, e.g.: Böttcher, C. J. F. *Theory of Electric Polarisation*; Elsevier: New York, 1952; pp 415–20.
- (4) Hashin, Z.; Shtrikman, S. *J. Appl. Phys.* **1962**, *33*, 3125.
- (5) Bergman, D. *J. Phys. Rev. B* **1976**, *14*, 1531.
- (6) Cohen, R. W.; Cody, G. D.; Coutts, D.; Abeles, B. *Phys. Rev. B* **1973**, *8*, 3689.
- (7) Ricard, D.; Roussignol, Ph.; Flytzanis, C. *Opt. Lett.* **1985**, *10*, 511.
- (8) Hache, F.; Ricard, D.; Flytzanis, C. *J. Opt. Soc. Am. B* **1986**, *3*, 1647.
- (9) Hache, F.; Ricard, D.; Flytzanis, C.; Kreibig U. *Appl. Phys. A* **1988**, *47*, 347.
- (10) Agarwal, G. S.; Dutta Gupta, S. *Phys. Rev. A* **1988**, *38*, 5678.
- (11) Sipe, J. E.; Boyd, R. W. *Phys. Rev. A* **1992**, *46*, 1614.
- (12) Stroud, D.; Hui, P. M. *Phys. Rev. B* **1988**, *37*, 8719.
- (13) Zeng, X. C.; Bergman, D. J.; Hui, P. M.; Stroud, D. *Phys. Rev. B* **1988**, *38*, 10970.
- (14) Bloemer, M. J.; Haus, J. W.; Ashley, P. R. *J. Opt. Soc. Am. B* **1990**, *7*, 790.
- (15) Bloemer, M. J.; Ashley, P. R.; Haus, J. W.; Kalyaniwalla, N.; Christensen, C. R. *IEEE J. Quantum Electron.* **1990**, *26*, 1075.
- (16) LaPeruta, R.; Van Wagener, E. A.; Roche, J. J.; Kittipichai, P.; Wnek, G. E.; Korenowski, G. M. *Proc. SPIE* **1991**, *1497*, 357.
- (17) Uchida, K.; Kaneko, S.; Omi, S.; Hata, C.; Tanji, H.; Asahara, Y.; Ikushima, A. J.; Tokizaki, T.; Nakamura, A. *J. Opt. Soc. Am. B* **1994**, *11*, 1236.
- (18) Haglund, R. F., Jr.; Yang, L.; Magruder, R. H., III; Wittig, J. E.; Becker, K.; Zehr, R. A. *Opt. Lett.* **1993**, *18*, 373.
- (19) Yang, L.; Becker, K.; Smith, F. M.; Magruder, R. H., III; Haglund, R. F., Jr.; Yang, L.; Dorsenville, R.; Alfano, R. R.; Zehr, R. A. *J. Opt. Soc. Am. B* **1994**, *11*, 457.
- (20) Magruder, R. H., III; Osborne, D. H., Jr.; Zehr, R. A. *J. Non-Cryst. Solids* **1994**, *176*, 299.
- (21) Magruder, R. H., III; Haglund, R. F., Jr.; Yang, L.; Wittig, J. E.; Becker, K.; Zehr, R. A. *Mater. Res. Soc. Symp. Proc.* **1992**, *244*, 369.
- (22) Magruder, R. H., III; Haglund, R. F., Jr.; Yang, L.; Wittig, J. E.; Zehr, R. A. *J. Appl. Phys.* **1994**, *76*, 708.
- (23) Haglund, R. F., Jr.; Yang, L.; Magruder, R. H., III; Becker, K.; Wittig, J. E.; White, C. W.; Zehr, R. A.; Yang, L.; Dorsenville, R.; Alfano, R. R. *Proc. SPIE* **1993**, *1852*, 113.
- (24) White, C. W.; Thomas, D. K.; Zehr, R. A.; McCallum, J. C.; Pogany, A.; Haglund, R. F., Jr.; Magruder, R. H., III; Yang, L. *Mater. Res. Soc. Symp. Proc.* **1992**, *268*, 331.
- (25) Efros, A. I. L.; Efros, A. L. *Sov. Phys. Semiconduct.* **1982**, *16*, 772.
- (26) Jain, R. K.; Lind, R. C. *J. Opt. Soc. Am.* **1983**, *73*, 647.
- (27) Roussignol, P.; Ricard, D.; Rustagi, K. C.; Flytzanis, C. *Opt. Commun.* **1985**, *55*, 143.
- (28) Yao, S. S.; Karaguleff, C.; Gabel, A.; Fortenberry, R.; Seaton, C. T.; Stegeman, G. I. *Appl. Phys. Lett.* **1985**, *46*, 801.
- (29) Olbright, G. R.; Peyghambarian, N. *App. Phys. Lett.* **1986**, *48*, 1184.
- (30) Olbright, G. R.; Peyghambarian, N.; Koch, S. W.; Banyai, L. *Opt. Lett.* **1987**, *12*, 413.
- (31) Hall, D. W.; Borrelli, N. F. *J. Opt. Soc. Am. B* **1988**, *5*, 1650.
- (32) Miller, D. A. B.; Chemla, D. S.; Schmitt-Rink, S. *Appl. Phys. Lett.* **1988**, *52*, 2154.
- (33) Remillard, J. T.; Wang, H.; Webb, M. D.; Steel, D. G. *IEEE J. Quantum Electron.* **1989**, *25*, 408.
- (34) Hache, F.; Ricard, D.; Flytzanis, C. *Appl. Phys. Lett.* **1989**, *55*, 1504.
- (35) Peyghambarian, N.; Fluegel, B.; Hulin, D.; Migus, A.; Joffre, M.; Antonetti, A.; Koch, S. W.; Lindberg, M. *IEEE J. Quantum Electron.* **1989**, *25*, 2516.
- (36) Ricard, D.; Roussignol, P.; Hache, F.; Flytzanis, C. *Phys. Status Solidi* **1990**, *159*, 275.
- (37) Roussignol, P.; Ricard, D.; Flytzanis, C. *Appl. Phys. B* **1990**, *51*, 437.
- (38) Zimin, L. G.; Gaponenko, S. V.; Lebed', V. Yu.; Malinovskii, I. E.; Germanenko, I. N. *J. Lumin.* **1990**, *46*, 101.
- (39) Morgan, R. A.; Park, S.; Koch, S. W.; Peyghambarian, N. *Semiconduct. Sci. Technol.* **1990**, *5*, 544.
- (40) Justus, B. L.; Tonucci, R. J.; Berry, A. D. *Appl. Phys. Lett.* **1992**, *61*, 3151.
- (41) Brus, L. *App. Phys. A* **1991**, *53*, 465.
- (42) Reisfeld, R. *Structure and Bonding*; Reisfeld, R., Jorgensen, C. K., Eds.; Springer-Verlag: New York, 1996; Vol. 85.
- (43) Alivisatos, A. P. *MRS Bull.* **1995**, *20*, 23.
- (44) Haus, J. W.; Inguva, R.; Bowden, C. M. *Phys. Rev. A* **1989**, *40*, 5729.
- (45) Haus, J. W.; Kalyaniwalla, N.; Inguva, R.; Bloemer, M.; Bowden, C. M. *J. Opt. Soc. Am. B* **1989**, *6*, 797.
- (46) Neeves, A. E.; Birnboim, M. H. *Opt. Lett.* **1988**, *13*, 1087.
- (47) Neeves, A. E.; Birnboim, M. H. *J. Opt. Soc. Am. B* **1989**, *6*, 787.
- (48) Zhang, X.; Stroud, D. *Phys. Rev. B* **1994**, *49*, 944.
- (49) Wang, J.; Li, Z. *Phys. Lett. A* **1995**, *199*, 199.
- (50) Zhou, H. S.; Honma, I.; Komiyama, H.; Haus, J. W. *Phys. Rev. B* **1994**, *50*, 12052.
- (51) Kalyaniwalla, N.; Haus, J. W.; Inguva, R.; Birnboim, M. H. *Phys. Rev. A* **1990**, *42*, 5613.
- (52) Bruggeman, D. A. G. *Ann. Phys. (Leipzig)* **1935**, *24*, 636.
- (53) Landauer, R. *J. Appl. Phys.* **1952**, *23*, 779.
- (54) Stroud, D. *Phys. Rev. B* **1975**, *12*, 3368.
- (55) Sheng, P. *Phys. Rev. Lett.* **1980**, *45*, 60.
- (56) Gittleman, J. I.; Abeles, B. *Phys. Rev. B* **1977**, *15*, 3273.
- (57) Grannan, D. M.; Garland, J. C.; Tanner, D. B. *Phys. Rev. Lett.* **1981**, *46*, 375.
- (58) Berthier, S.; Driss-Khodja, K.; Lafait, J. *J. Phys.* **1987**, *48*, 601.
- (59) Stroud, D.; Zhang, X. *Physica A* **1994**, *207*, 55.
- (60) Zhou, M.; Sheng, P.; Chen, Z.; Chui, S. T. *Appl. Opt.* **1991**, *30*, 145.
- (61) Boyd, R. W.; Sipe, J. E. *J. Opt. Soc. Am. B* **1994**, *11*, 297.
- (62) Fischer, G. L.; Boyd, R. W.; Gehl, R. J.; Jenekhe, S. A.; Osaheni, J. A.; Sipe, J. E.; Weller-Brophy, L. A. *Phys. Rev. Lett.* **1995**, *74*, 1871.
- (63) Sheik-Bahae, M.; Said, A. A.; Wei, T.; Hagan, D. J.; Van Stryland, E. W. *IEEE J. Quantum Electron.* **1990**, *26*, 760.
- (64) Gehr, R. J.; Fischer, G. L.; Boyd, R. W.; Sipe, J. E. *Phys. Rev. A*, in press.
- (65) Levy, O.; Yagil, Y.; Bergman, D. J. *J. Appl. Phys.* **1994**, *76*, 1431.
- (66) Bergman, D. J.; Levy, O.; Stroud, D. *Phys. Rev. B* **1994**, *49*, 129.
- (67) Chui, S. T.; Zhou, M. Y.; Sheng, P.; Chen, Z. *J. Appl. Phys.* **1991**, *69*, 3366.
- (68) Markel, V. A.; Shalaev, V. M.; Stechel, E. B.; Kim, W.; Armstrong, R. L. *Phys. Rev. B* **1996**, *53*, 2425.
- (69) Berry, M. V.; Percival, I. C. *Opt. Acta* **1986**, *33*, 577.
- (70) Hui, P. M.; Stroud, D. *Phys. Rev. B* **1986**, *33*, 2163.
- (71) Shalaev, V. M.; Stockman, M. I. *Z. Phys. D* **1988**, *10*, 71.
- (72) Markel, V. A.; Muratov, L. S.; Stockman, M. I.; George, T. F. *Phys. Rev. B* **1991**, *43*, 8183.
- (73) Butenko, A. V.; Shalaev, V. M.; Shtokman, M. I. *Sov. Phys. JETP* **1988**, *67*, 60.
- (74) Butenko, A. V.; Shalaev, V. M.; Stockman, M. I. *Z. Phys. D* **1988**, *10*, 81.
- (75) Rautian, S. G.; Safonov, V. P.; Chubakov, P. A.; Shalaev, V. M.; Shtokman, M. I. *JETP Lett.* **1988**, *47*, 243.
- (76) Butenko, A. V.; Chubakov, P. A.; Danilova, Yu. E.; Karpov, S. V.; Popov, A. K.; Rautian, S. G.; Safonov, V. P.; Slabko, V. V.; Shalaev, V. M.; Stockman, M. I. *Z. Phys. D* **1990**, *17*, 283.
- (77) Shalaev, V. M.; Botet, R.; Jullien, R. *Phys. Rev. B* **1991**, *44*, 12216.
- (78) Shalaev, V. M.; Stockman, M. I.; Botet, R. *Phys. A* **1992**, *185*, 181.
- (79) Stockman, M. I.; George, T. F.; Shalaev, V. M. *Phys. Rev. B* **1991**, *44*, 115.
- (80) Shalaev, V. M.; Moskovits, M.; Golubentsev, A. A.; John, S. *Phys. A* **1992**, *191*, 352.
- (81) Stockman, M. I.; Shalaev, V. M.; Moskovits, M.; Botet, R.; George, T. F. *Phys. Rev. B* **1992**, *46*, 2821.
- (82) Shalaev, V. M.; Poliakov, E. Y.; Markel, V. A. *Phys. Rev. B* **1996**, *53*, 2437.
- (83) Yu, K. W.; Chan, E. M. Y.; Chu, Y. C.; Gu, G. Q. *Phys. Rev. B* **1995**, *51*, 11416.
- (84) Yu, K. W. *J. Phys.: Condens. Matter* **1995**, *7*, 3355.
- (85) Choy, T. S.; Yu, K. W. *Phys. Rev. B* **1995**, *52*, 3341.
- (86) Choy, T. S.; Yu, K. W. *Phys. Lett. A* **1995**, *202*, 129.
- (87) Clerc, J. P.; Giraud, G.; Laugier, J. M.; Luck, J. M. *Adv. Phys.* **1990**, *39*, 191.